Investigation of the Effect of Cu-Based Catalyst Acidity on Hydrogen Production from the Water-Gas Shift Reaction

Khandan, Nahid*[*+]*, Mashayekhi, Maziyar

Department of Chemical Technologies, Iranian Research Organization for Science and Technology, Tehran, I.R. IRAN

ABSTRACT: *The Water Gas Shift reaction is essential to numerous activities, including the production of Hydrogen and the reforming of natural gas. This reaction is enhanced by various catalysts. However, the catalyst acidity is a crucial parameter that affects catalyst performance. In this work, using the co-precipitation method, the effects of catalyst acidity on the low-temperature Water Gas Shift (WGS) reaction were examined. In this way, ternary Cu/ZnO/ZrO_2 and Cu/ZnO/Al_2O_3 catalysts were selected and made. XRD, SEM, BET, NH_3-TPD, CO-TPD, and TGA studies were used to characterize the catalysts. The catalytic performance was tested at atmospheric pressure, 180 ℃, and space velocity 3600 /h, with the inlet gas composition H_2O/CO= 1/1 in a fixed bed micro-reactor for around 6 hours. Weak and moderately acidic sites were shown to be preferable to strong sites for the water gas shift reaction. The Cu/ZnO/ZrO_2 catalyst was the best one to use in the WGS process because of its acidity, which mostly consisted of mildly acidic sites. Based on the experimental results, Cu/ZnO/ZrO_2 had a hydrogen selectivity and conversion of around 61% and 98%, respectively.*

KEYWORDS: *Water Gas Shift reaction, Catalyst acidity, Cu/ZnO/ZrO_2 catalyst, Cu/ZnO/Al_2O_3 catalyst.*

INTRODUCTION

In recent years, due to the significant reduction of fossil fuel sources, hydrogen-based processes have become particularly important as an alternative to fossil fuels [1,2]. This fact has led scientists to develop new methods to produce and apply Hydrogen as a clean and abundant energy resource [3–7]. Renewable technologies such as Proton Exchange Membrane Fuel Cells (PEMFCs) are being investigated as viable replacements for high-emission combustion engines in this area [8–11]. Hydrogen is the primary feedstock of PEMFCs. It is produced by the reforming Hydrocarbons. However, the product has some impurities, such as Carbon monoxide (1-10 vol. %). The sensibility of Carbon Monoxide poisoning is one of the main problems of Proton Exchange Membrane Fuel cells. Carbon Monoxide is adsorbed on PEMFCs electrode as a catalyst poison [12–15].

The water gas shift reaction is a significant reaction that can collaborate with the efficiency of fuel cells by increasing hydrogen production and decreasing carbon monoxide concentration [16–19]. Eq. (1) is the chemical reaction followed by the water-gas shift reaction [20].

$$H_2O + CO \rightarrow H_2 + CO_2 \qquad (1)$$

$$\Delta HR = -41.2 \text{ kJ/mol} \qquad \Delta G = -28.6 \text{ kJ/mol}$$

The process is split into two parts based on the temperature at which it works: the low-temperature water

* *To whom correspondence should be addressed.*
+ E-mail: khandan@irost.org
1021-9986/2023/11/3728-3736 9/$/5.09

gas shift reaction and the high-temperature water gas shift reaction [21]. However, these reactions are slow reactions that need to accelerate by using a catalyst. Many studies have been done to find the appropriate catalyst for each region [12,14, 22–25]. Among all materials, copper is a good candidate for low-temperature regions [10,12,14,18, 26–31]. To reduce the amount of carbon monoxide, catalysts must be made that are very active at low temperatures, where the equilibrium for removing carbon monoxide with the water–gas shift reaction is good [32–36].

The stability of the catalyst is another crucial element that affects the catalyst's lifetime and the process. Consequently, it should be considered, especially wherever carbon monoxide is present. Coke formation is one of the main side reactions that may occur during the CO removal by water-gas shift reaction, poisoning the catalyst and acting as a reaction inhibitor [37]. Eq. (2) is Carbon monoxide conversion to coke according to the Boudouard reaction [38].

$$2\,CO \leftrightarrow CO_2 + C \qquad (2)$$

This reaction shows that Coke can be produced over the catalyst, and consequently, the activity of the catalyst may be reduced [39–41]. So, much research has focused on finding ways to prevent coke formation during specific chemical reactions by modifying the surface structure of the catalyst [42–44]. Several studies have been carried out on the effect of catalyst acidity on various process efficiency. By investigating the impact of ZSM5 catalysts acidity on the reaction of Propylene production from Hexane cracking, Sun and his colleagues found that increasing the concentration of strong Brønsted acid sites leads to an increase in the production of undesirable side products, including coke, and as a result, decreases the selectivity and efficiency of the main reaction [45]. *Lee et al*. showed that the acidity of the HY catalyst plays an essential role in the selective ring opening reaction of multi-ring aromatics in heavy oil, and there is an optimum value for catalyst acidity in each reaction [46]. In another study, Jensen and Sigman evaluated the effect of catalyst acidity in a hydrogen bond-catalyzed reaction. They observed a linear relationship between surface acidity and both reaction rate and selectivity [47]. *Jian-Lu et al*. showed that the catalytic activity of palladium-supported catalysts is strongly dependent on surface acidity and has a direct relationship with it [48]. *Viscardi et al*. also investigated the effect of the strength of surface acid sites on the activity and deactivation of the silica-alumina catalysts in the conversion of methanol to dimethyl ether. They found that the Brønsted and Lewis acid sites with medium strength are required to achieve the appropriate conversion rate [49].

A recent study on the effect of surface acidity on catalyst performance and, as a result, coke production is available. We tried to study the coke formation and the essential characteristic of a catalyst that enhances this phenomenon. In this way, two catalysts, including $Cu/ZnO/Al_2O_3$ and $Cu/ZnO/ZrO_2$, were selected as case studies. $Cu/ZnO/Al_2O_3$ is a common catalyst for many catalytic processes, especially the water gas shift reaction. However, it may not be the best candidate for the water gas shift process. In this research, $Cu/ZnO/Al_2O_3$ and $Cu/ZnO/ZrO_2$ catalysts were prepared and compared together.

EXPERIMENTAL SECTION

Catalyst preparation

The co-precipitation method was used to create the catalysts. An aqueous solution of Na_2CO_3 (1 M) was added dropwise to a solution of metal nitrates while stirring continuously at 60 ℃. The solution of metal nitrates contained the desired amounts of $M(NO_3)_2$ (M = Cu, Zn) and Al $(NO_3)_3.9H_2O$ or $ZrO(NO_3)_2{\cdot}xH_2O$ with a total cation concentration of 1M and the weight ratio of 20/10/70 for Cu/ZnO/Metal oxide. The pH of the suspension was measured using a pH meter, and the Na_2CO_3 solution was injected at a regulated rate to keep the pH of the suspension at the desired level (about 6) throughout precipitation. The residue was stirred for 90 min, aged at room temperature for 30 minutes, filtered three times, and then washed for 15 minutes between each filtration. The residue was then dried for 14 hours at 110 ℃ and calcined for 4 hours by airflow at a progressive temperature increase up to 400 °C [50].

Catalyst Characterization

APW-1800 Philips X-ray diffractometer with Cu K radiation and a wavelength of 1.54Å was employed for X-ray measurement. At 40 kV and 40 mA, spectra were measured with a step size of 0.02 across a 2 range of 4° to 90°. Using the Scherrer equation, the CuO crystal sizes of the calcined catalysts were calculated from the whole width at half maximum of the CuO X-ray peaks.

Using Micro Meritics ASAP2010 equipment, the BET surface areas of the catalysts were determined using a multipoint N_2 adsorption-desorption technique at liquid N_2

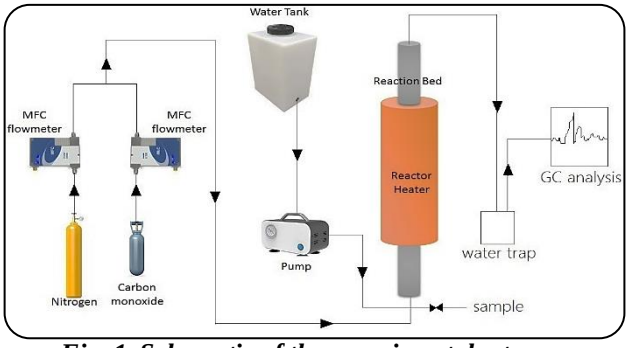

Fig. 1. Schematic of the experimental setup

temperature (77 K). Before analysis, samples were out-gassed under a vacuum to remove the physisorbed water. A catalyst weight of 5 mg was used for the ThermoGravimetric Analysis (TGA), carried out in an environment of 10 vol% Ar (100 mL/h) at a slow heating rate of 10 °C/min up to 800 °C. The weight losses of the manufactured catalysts due to coke depletion was evaluated to assess their stability.

SEM was used to examine the microstructures of the produced catalysts using a field emission electron microscope (Philips, XL30) running at 15.0 kV. Using an EDX Link Analytical QX 2000 spectrometer connected to a scanning electron microscope, Energy-Dispersive X-ray Spectroscopy (EDS) was used to evaluate the elemental composition of the catalysts.

Acidity measurements were made using standard flow equipment with a Thermal Conductivity (TC) detector and temperature-programmed desorption of ammonia (NH_3-TPD). The sample was processed for 1 hour at 500 °C in flowing helium, cooled to 150 °C, and then exposed for 30 minutes to NH_3 (20 mL/min). To eliminate the physisorbed NH_3, samples were purged with He for 1 hour at the same temperature. The TPD measurements were carried out in flowing He (30 mL/min) at a heating rate of 10 °C/min from 100 to 700 °C [51].

Al_2O_3 and ZrO_2 were subjected to CO-TPD analysis. In a manner comparable to NH_3-TPD analysis, this study was conducted. As a result, 100 mg of each sample were processed for 1 hour at 500 °C under flowing helium, cooled to 150 °C, and then exposed to CO for 30 minutes at a rate of 20 mL/min. After that, samples were purged with He for 1 hour at the same temperature to eliminate the physisorbed CO. The TPD measurements were carried out in flowing He (30 mL/min) at a heating rate of 10 °C/min from 100 to 700 °C.

Catalytic reactions

In a fixed bed, 3-mm-diameter tubular stainless steel micro-reactor with 500 mg of catalyst, experiments on catalyst performance were conducted for 6 hours at atmospheric pressure and 180 °C. Fig. 1 depicts a schematic of the experimental setup. The micro-reactor was equipped with an electrical furnace coil and PID controller. The flows of high-purity CO and Nitrogen were controlled by mass flow controllers and directed to the bottom of the reactor. Before the catalytic activity measurements, the catalysts would be reduced by Hydrogen flow at normal pressure. For this purpose, first, the reactor was flushed with Nitrogen, and heated from room temperature to 400 °C and then a mixed gas flow having the composition of N_2/H_2= 1/1 with a flow rate of 60 mL/min was subjected to the reactor for 6 h. A feed gas containing H_2O/CO (molar ratio= 1/1) with gas hourly space velocity (GHSV) of 3600 /h was used for all experiments.

A calibrated water pump injected water into the flowing gas stream, which was then heated in the gas feed line before entering the reactor. A small portion of the reactor effluent (after passing through a trap for removing water) was subjected to a Philips PU4815 Gas Chromatography (GC). It was continuously analyzed with two TCDs, the first, to investigate Hydrogen and the second to measure Carbon Monoxide. The following equations were used to determine the activity and selectivity of catalysts:

$$\text{CO conversion} = \frac{\text{Inlet molar flow rate of CO} - \text{Outlet molar flow rate of CO}}{\text{Inlet molar flow rate of CO}} \quad (3)$$

$$H_2/CO_2 \text{selectivity} = \frac{\text{Molar flow rate of H2/CO2 production}}{\text{Inlet molar flow rate of CO} - \text{Outlet molar flow rate of CO}} \quad (4)$$

RESULTS AND DISCUSSION

Characterization of the catalysts

The XRD patterns of synthesized catalysts are shown in Fig. 2. This graph shows how well-prepared the catalysts are. As can be seen, the crystallite phase of CuO has three prominent peaks that are recognizable at 2θ=31.9 and 35.5° and 38.7°, whose Miller indices are {110}, {111}, and {200}, respectively. Miller indices are written using JCPDS card number 00-041-0254 for the Mono clinic structure of copper oxide. These peak intensities are the largest in the prepared sample. The most intense peak

Table 1: Characterization of fabricated catalysts

Catalyst	$Cu/ZnO/Al_2O_3$	$Cu/ZnO/ZrO_2$
Surface Area (m^2/g)	38.397	64.696

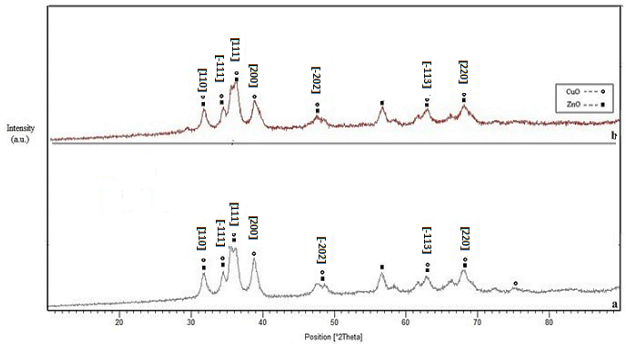

Fig. 2: XRD patterns of the fabricated catalysts: a) Cu/ZnO /Al_2O_3, b) Cu/ZnO /ZrO_2

observed for ZnO was located at 2θ=56.8° with a Miller index of {110} according to JCPDS card number 00-036-1451 for the hexagonal structure of zinc oxide. Each catalyst's Cu crystallite size was calculated using the Debye-Scherrer equation (Eq. (5)). According to this equation, the crystal sizes of the catalysts are computed from the whole width at half maximum of the X-ray peaks.

$$D = \frac{K\lambda}{\beta \cos \theta} \quad (5)$$

Where θ is the diffracting angle, λ is the X-ray wavelength equal to 1.54 Å, constant k equals 0.9, and is the entire width of a diffraction peak at half maximum intensity (FWHM). The average Cu crystallite sizes were calculated at 17.73 nm and 6.60 nm for ZrO_2 and Al_2O_3-based catalysts, respectively.

Table 1 indicates the results of the BET analysis. It is observed that the surface area of the *Cu/ZnO/ZrO_2* catalyst is significantly higher than the other catalyst. This means that the dispersion of active sites (*Cu*) in the *Cu/ZnO/ZrO_2* catalyst is better than that of the *Cu/ZnO/Al_2O_3* catalyst, and consequently, the catalytic performance is higher.

Fig. 3 gives the SEM images. It seems that the crystals are spherical. Furthermore, the manufactured catalysts' particle sizes, as determined by SEM, are roughly equivalent.

Activity tests

Fig. 4 shows the conversion of carbon monoxide over time on stream for both catalysts. This figure demonstrates that the $Cu/ZnO/ZrO_2$ catalyst has higher activity than the $Cu/ZnO/Al_2O_3$ catalyst. Moreover, the activity of

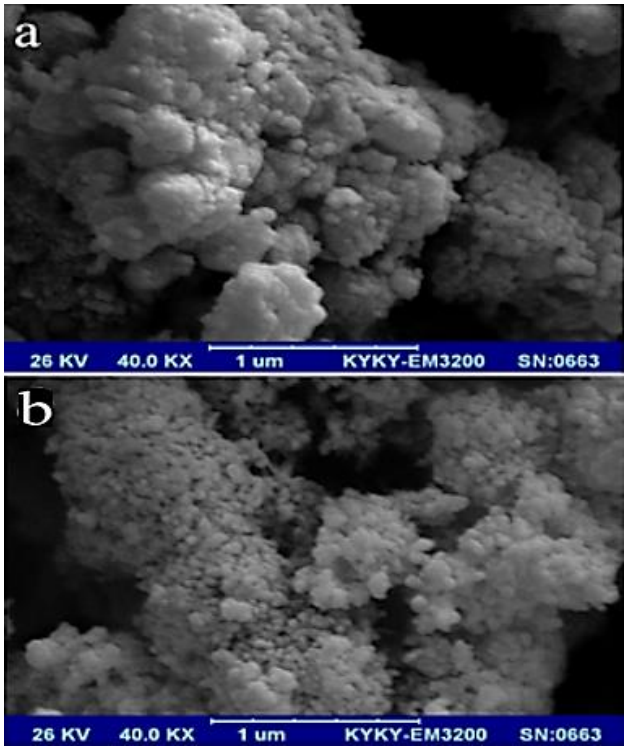

Fig. 3: SEM images of the fabricated catalysts: a) Cu/ZnO/Al_2O_3, b) Cu/ZnO/ZrO_2

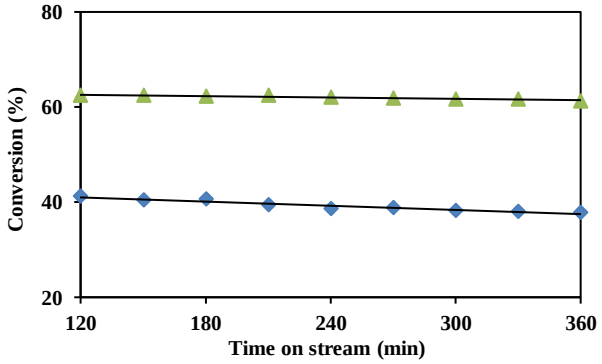

Fig. 4: Conversion profiles of Carbon monoxide on fabricated catalysts: ▲ Cu/ZnO/ZrO_2, ◆Cu/ZnO/Al_2O_3

the $Cu/ZnO/Al_2O_3$ catalyst reduces over time. Higher activity may be due to the higher dispersion of Cu active sites on the $Cu/ZnO/ZrO_2$. This confirms the results of the BET analysis. The reduction of the $Cu/ZnO/Al_2O_3$ catalyst's activity can be due to coke formation. Characteristics and surface structure of a heterogeneous catalyst influence the ratios and type of the products in chemical processes, the yields of chemical reactions, the percentage of adsorption, the formation of intermediate reactants, and some undesirable products that poison the active catalytic sites

Table 2: Results of thermal gravimeter analysis over the used catalysts (after six hours of reactor test)

catalyst	Weight loss (%)
$Cu/ZnO/ZrO_2$	0.5
$Cu/ZnO/Al_2O_3$	2.1

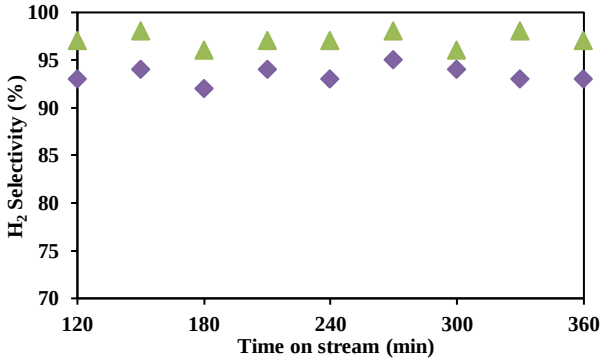

Fig. 5: Profiles of H_2 selectivity obtained by using the fabricated catalysts: ▲ $Cu/ZnO/ZrO_2$, ◆ $Cu/ZnO/Al_2O_3$

and, following that reduces the catalyst activity. In other words, another reaction, namely the Boudouard reaction (2), may be occurred at the process condition. At high temperatures, the exothermic nature of this process causes it to reverse. The ratio of CO_2/CO gases in the outlet depends on temperature and the applied catalyst.

Fig. 5 shows the selectivity of Hydrogen obtained from applied catalysts. This figure indicates that the Hydrogen selectivity of $Cu/ZnO/Al_2O_3$ is lower than the other. It can be said $Cu/ZnO/Al_2O_3$ accelerates the Boudouard reaction and causes some carbon monoxide to convert to Carbon dioxide and coke according to formula (4). The results of the thermal gravimeter analysis are given in Table 2. According to the temperature program, this study was conducted in an argon environment between room temperature and 800°C while increasing 20 °C/min. Weight loss at the temperature range of 500°C to 800°C was related to carbon delivery. Table 2 shows that coke is formed during the water gas shift reaction. However, this phenomenon is critical when $Cu/ZnO/Al_2O_3$ is applied as the main reaction catalyst.

NH_3-TPD was utilized to characterize the surface acidity of heterogeneous catalysts. Results are given in Fig. 6. The peaks indicate the acidic strength of the catalysts; lower than 200 °C, between 200 °C to 400 °C, and higher than 400 °C are related to weak, medium, and strong acidic sites, respectively. As shown in Fig. 6, $Cu/ZnO/Al_2O_3$ has a strong acidic site. This means

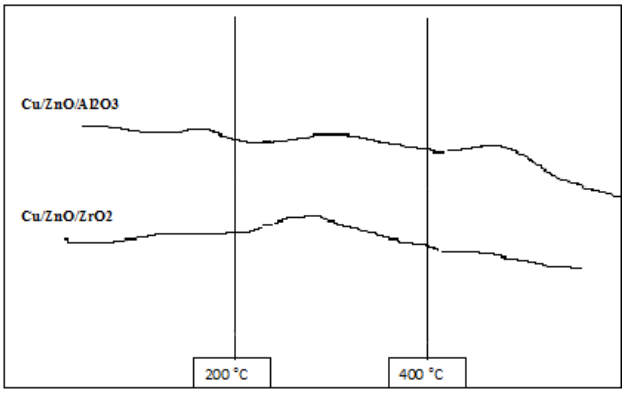

Fig. 6: NH_3-TPD profiles of the fabricated catalysts

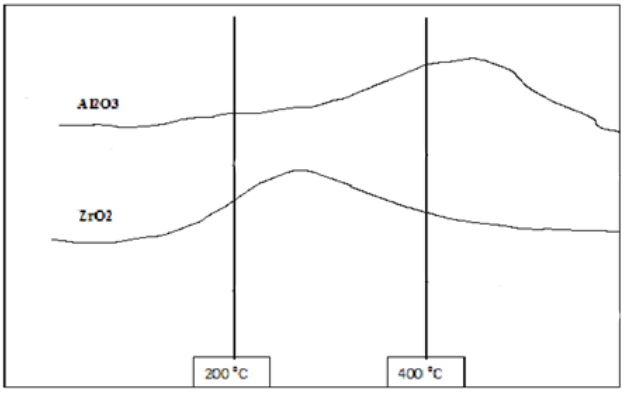

Fig. 7: CO-TPD profiles of the supports

The adsorption of carbon monoxide on the $Cu/ZnO/Al_2O_3$ surface is irreversible, and enhancing the conversion of Carbon monoxide to carbon. On the other hand, carbon deposits on the catalyst surface due to low process temperature (180°C) and covers gradually active sites. This reduces the conversion of Carbon monoxide during the time on stream. According to Fig. 6, this phenomenon is less critical for other catalysts.

To know the effect of acidic sites of catalyst support, CO –TPD analysis was performed solely on ZrO_2 and Al_2O_3. Results are given in Fig. 7. It confirms the results of NH_3-TPD. It is observed that the adsorption of Carbon monoxide on supports is different. Al_2O_3 adsorbs carbon monoxide very strongly, while adsorption on ZrO_2 is medium. It can be concluded that strong acidic sites enhance the conversion of Carbon monoxide to coke.

In other words, the number of acidic sites is also significant. According to Figure 6, it is observed that Zirconia has more acidic sites. Therefore, it is deemed that acidic sites enhance the water gas shift reaction. However, strong acidic sites are not sufficient due to accelerating coke formation.

CONCLUSIONS

Carbon monoxide was converted to hydrogen by using supported copper catalysts. The surface acidity was changed by changing the catalyst support from alumina to zirconium oxide. The NH_3-TPD and CO-TPD analysis confirmed the change in surface acidity intensity. The acidic strength of the catalyst has an influential role in the water gas shift process. Weak and medium acidic strength enhances the conversion of Carbon monoxide to Hydrogen. In contrast, strong acidic sites lead to irreversible carbon monoxide adsorption on the surface and enhance the Boudouard reaction and, consequently coke formation. Based on this foundation, $Cu/ZnO/ZrO_2$ catalyst was a better candidate than $Cu/ZnO/Al_2O_3$, to be applied in Water Gas Shift (WGS) reaction due to its acidity, which had mainly moderate acidic sites. The conversion and hydrogen selectivity of $Cu/ZnO/ZrO_2$ were around 61% and 98% after 6 hours of experiment, respectively.

Nomenclatures

carbon monoxide	CO
gas hourly space velocity	GHSV
scanning electron microscopy	SEM
X-ray Diffraction	XRD
Joint Committee on Powder Diffraction Standards card	JCPDS card
water gas shift	WGS

ACKNOWLEDGEMENTS

The financial support of the Iran National Science Foundation (INSF), contract no. 91/S/23551, is gratefully acknowledged.

Received: Mar. 15, 2023; Accepted: Jun. 12, 2023

REFERENCES

[1] Mousavi-Salehi S., Keshipour S., Ahour F., Gold Supported on Graphene Oxide/Silica Photocatalyst for Hydrogen Generation from Formic Acid, *Journal of Physics and Chemistry of Solids*, **176:** 111239 (2023).

[2] Eyvari-Ashnak F., Keshipour S., Amines Functionalities on Chitosan Boasting Photocatalytic Activity of Cobalt(II)-Phthalocyanine in Water-Splitting, *Molecular Catalysis*, **534:** 112820 (2023).

[3] Al-Azmi A., Keshipour S., New Bidental Sulfur-Doped Graphene Quantum Dots Modified with Gold as a Catalyst for Hydrogen Generation, *Journal of Colloid and Interface Science*, **612:** 701–9 (2022).

[4] Keshipour S., Asghari A., A Review on Hydrogen Generation by Phthalocyanines, *International Journal of Hydrogen Energy*, **47:** 12865–12881 (2022).

[5] Keshipour S., Mohammad-Alizadeh S., Razeghi M.H., Copper Phthalocyanine@Graphene Oxide as a Cocatalyst of TiO_2 in Hydrogen Generation, *Journal of Physics and Chemistry of Solids*, **161:** 110434 (2022).

[6] Keshipour S., Mohammad-Alizadeh S., Nickel Phthalocyanine@Graphene Oxide/TiO_2 as an Efficient Degradation Catalyst of Formic Acid Toward Hydrogen Production, *Scientific Reports*, **11:** 1–8 (2021).

[7] Khani H., Khandan N., Eikani M. H., Eliassi A., Production of Clean Hydrogen Fuel on a Bifunctional Iron Catalyst via Chemical Loop Reforming of Methanol, *Fuel*, **334:** 126607 (2023).

[8] Tabakova T., Idakiev V., Papavasiliou J., Avgouropoulos G., Ioannides T., Effect of Additives on the WGS Activity of Combustion Synthesized CuO/CeO_2 Catalysts, *Catalysis Communications*, **8:** 101–6 (2007).

[9] Shafiee S., Topal E., When will Fossil Fuel Reserves be Diminished?, *Energy Policy*, **37:** 181–9 (2009).

[10] Montazeri-Gh M., Mahmoodi-k M., Development a New Power Management Strategy for Power Split Hybrid Electric Vehicles, *Transportation Research Part D: Transport and Environment*, **37:** 79–96 (2015).

[11] Andrews J., Shabani B., Re-Envisioning the Role of Hydrogen in a Sustainable Energy Economy, *International Journal of Hydrogen Energy*, **37:** 1184–1203 (2012).

[12] Li Z., Li N., Wang N., Zhou B., Yu J., Song B., et al., Metal-Support Interaction Induced ZnO Overlayer in $Cu@ZnO/Al_2O_3$ Catalysts Toward Low-Temperature Water-Gas Shift Reaction, *RSC Advances*, **12:** 5509–5516 (2022).

[13] Zhang Z., Chen X., Kang J., Yu Z., Tian J., Gong Z., et al., The Active Sites of Cu–ZnO Catalysts for Water Gas Shift and CO Hydrogenation Reactions, *Nature Communications*, **12:** 1–9 (2021).

[14] Dasireddy V., Rubin K., Pohar A., Likozar B., Surface Structure–Activity Relationships of $Cu/ZnGaO_X$ Catalysts in Low Temperature Water–Gas Shift (WGS) Reaction for Production of Hydrogen Fuel, *Arabian Journal of Chemistry*, **13:** 5060–5074 (2020).

[15] Li L., Song L., Wang H., Chen C., She Y., Zhan Y., et al., Water-Gas Shift Reaction over CuO/CeO_2 Catalysts: Effect of CeO_2 Supports Previously Prepared by Precipitation with Different Precipitants, *Inter. J. Hydrogen Energy*, **36:** 8839–8849 (2011).

[16] Ilieva L., Petrova P., Ivanov I., Munteanu G., Boutonnet M., Sobczac J.W., et al., Nanosized Gold Catalysts on Pr-Modified Ceria for Pure Hydrogen Production via WGS Reaction, *Materials Chemistry and Physics*, **157:** 138–146 (2015).

[17] Silva L., Freitas M.M., Terra L.E., Coutinho A., Passos F.B., Preparation of $CuO/ZnO/Nb_2O_5$ Catalyst for the Water-Gas Shift Reaction, *Catalysis Today*, **344:** 59–65 (2020).

[18] De Oliveira Campos B.L., Delgado K.H., Wild S., Studt F., Pitter S., Sauer J., Surface Reaction Kinetics of the Methanol Synthesis and the Water Gas Shift Reaction on $Cu/ZnO/Al_2O_3$, *Reaction Chemistry and Engineering*, **6:** 868–87 (2021).

[19] De Oliveira C.S., Teixeira Neto É., Mazali I.O., Stabilization and Au Sintering Prevention Promoted by ZnO in CeOx–ZnO Porous Nanorods Decorated with Au Nanoparticles in the Catalysis of the Water-Gas Shift (WGS) Reaction, *Journal of Alloys and Compounds*, **892:** 162179 (2022).

[20] Wang C.W., Peng X.L., Liu J.Y., Jiang R., Li X.P., Liu Y.S., et al, A Novel Formulation Representation of the Equilibrium Constant for Water Gas Shift Reaction, *International Journal of Hydrogen Energy*, **47:** 27821–38 (2022).

[21] Pal D.B., Chand R., Upadhyay S.N., Mishra P.K., Performance of Water Gas Shift Reaction Catalysts: A Review, *Renewable and Sustainable Energy Reviews*, **93:** 549–65 (2018).

[22] Price C., Pastor-Pérez L., le Saché E., Sepúlveda-Escribano A., Reina T.R., Highly Active Cu-ZnO Catalysts for the WGS Reaction at Medium–High Space Velocities: Effect of the Support Composition, *International Journal of Hydrogen Energy*, **42:** 10747–51 (2017).

[23] Dongil A.B., Pastor-Pérez L., Escalona N., Sepúlveda-Escribano A., Carbon Nanotube-Supported $Ni-CeO_2$ Catalysts. Effect of the Support on the Catalytic Performance in the Low-Temperature WGS Reaction, *Carbon*, **101:** 296–304 (2016).

[24] Pérez P., Soria M.A., Carabineiro S.A.C., Maldonado-Hódar F.J., Mendes A., Madeira L.M., Application of Au/TiO_2 Catalysts in the Low-Temperature Water-Gas Shift Reaction, *International Journal of Hydrogen Energy*, **41:** 4670–81 (2016).

[25] Mao D., Zhang J., Zhang H., Wu D., A Highly Efficient Cu-ZnO/SBA-15 Catalyst for CO_2 Hydrogenation to CO under Atmospheric Pressure, *Catalysis Today*, **402:** 60–66 (2022).

[26] Xu L., Peng D., Liu W., Feng Y., Hou Y., Li X., et al., A Modified Co-precipitation Method to Prepare $Cu/ZnO/Al_2O_3$ Catalyst and Its Application in Low Temperature Water-gas Shift (LT-WGS) Reaction, *Journal Wuhan University of Technology, Materials Science Edition*, **33:** 876–83 (2018).

[27] Arbeláez O., Reina T.R., Ivanova S., Bustamante F., Villa A.L., Centeno M.A., et al., Mono and Bimetallic Cu-Ni Structured Catalysts for the Water Gas Shift Reaction, *Appl. Catalysis A: General*, **497:** 1–9 (2015).

[28] Jeong D.W., Na H.S., Shim J.O., Jang W.J., Roh H.S., Jung U.H., et al., Hydrogen Production from Low Temperature WGS Reaction on co-Precipitated $Cu-CeO_2$ Catalysts: An Optimization of Cu Loading, *International Journal of Hydrogen Energy*, **39:** 9135–42 (2014).

[29] Rad A.R.S., Khoshgouei M.B., Rezvani S., Rezvani A.R., Study of $Cu-Ni/SiO_2$ Catalyst Prepared from a Novel Precursor, $[Cu(H_2O)_6][Ni(dipic)_2].2H_2O/SiO_2$, for Water Gas Shift Reaction, *Fuel Processing Technology*, **96:** 9–15 (2012).

[30] Gamboa-Rosales N.K., Ayastuy J.L., González-Marcos M.P., Gutiérrez-Ortiz MA, Effect of Au Promoter in CuO/CeO_2 Catalysts for the Oxygen-Assisted WGS Reaction, *Catalysis Today*, **176:** 63–71 (2011).

[31] Rafiee M., Khandan N., Khorashe F. , Saffary S., Investigation of the Synthesis and Reactor Evaluation of Alumina- Supported Cu Catalysts on CO Conversion in a WGS Reaction, *Iranian Journal of Chemistry and Chemical Engineering (IJCCE)*, **42(5):** 1478-1490 (2023).

[32] Boukha Z., Ayastuy J.L., González-Velasco J.R., Gutiérrez-Ortiz M.A., Water-Gas Shift Reaction over a Novel Cu-ZnO/HAP Formulation: Enhanced Catalytic Performance in Mobile Fuel Cell Applications, *Applied Catalysis A: General*, **566:** 1–14 (2018).

[33] Huang C., Zhu C., Zhang M., Chen J., Fang K., Design of Efficient ZnO/ZrO_2 Modified CuCoAl Catalysts for Boosting Higher Alcohol Synthesis in Syngas Conversion, *Applied Catalysis B: Environmental*, **300:** 120739 (2022).

[34] Reina T.R., Ivanova S., Centeno M.A., Odriozola J.A., The Role of Au, Cu, and CeO_2 and Their Interactions for an Enhanced WGS Performance, *Applied Catalysis B: Environmental*, **187:** 98–107 (2016).

[35] Pastor-Pérez L., Buitrago-Sierra R., Sepúlveda-Escribano A., CeO_2-Promoted Ni/Activated Carbon Catalysts for the Water-Gas Shift (WGS) Reaction, *International Journal of Hydrogen Energy*, **39:** 17589–99 (2014).

[36] Zaherian A., Kazemeini M., Aghaziarati M., Alamolhoda S., Synthesis of Highly Porous Nanocrystalline Alumina as a Robust Catalyst for Dehydration of Methanol to Dimethyl Ether, *Journal of Porous Materials*, **20:** 151–7 (2013).

[37] Kayal S., Sun B., Chakraborty A., Study of Metal-Organic Framework MIL-101 (Cr) for Natural Gas (Methane) Storage and Compare with other MOFs (Metal-Organic Frameworks), *Energy*, **91:** 772–81 (2015).

[38] Wang C., Liu C., Fu W., Bao Z., Zhang J., Ding W., et al, The Water-Gas Shift Reaction for Hydrogen Production from Coke oven Gas over Cu/ZnO/Al_2O_3 Catalyst, *Catalysis Today*, **263:** 46–51 (2016).

[39] Tian P., Zhan G., Tian J., Tan K.B., Guo M., Han Y., et al, Direct CO_2 Hydrogenation to Light Olefins over $ZnZrO_x$ Mixed with Hierarchically Hollow SAPO-34 with Rice Husk as Green Silicon Source and Template, *Applied Catalysis B: Environmental*, **315:** 121572 (2022).

[40] Gao X., Cai P., Wang Z., Lv X., Kawi S., Surface Acidity/Basicity and Oxygen Defects of Metal Oxide: Impacts on Catalytic Performances of CO_2 Reforming and Hydrogenation Reactions, *Topics in Catalysis*, **22:** 38–51 (2022).

[41] Tande L.N., Resendiz-Mora E., Dupont V., Twigg M.V., Autothermal Reforming of Acetic Acid to Hydrogen and Syngas on Ni and Rh Catalysts, *Catalysts*, **11:** 1504 (2021).

[42] Wang J., Chen Y., Liu C., Lu Y., Lin X., Hou D., et al., Highly Stable Mo-based Bimetallic Catalysts for Selective Deoxygenation of Oleic Acid to Fuel-Like Hydrocarbons, *Journal of Environmental Chemical Engineering*, **11:** 109104 (2023).

[43] Cao X., Ai T., Xu Z., Lu J., Chen D., He D., et al., Insights into the Different Catalytic Behavior between Ce and Cr Modified MCM-41 Catalysts: Cr_2S_3 as New Active Species for CH_3SH Decomposition, *Separation and Purification Technology*, **307:** 122742 (2023).

[44] Gan Y., Lv Q., Li Y., Yang H., Xu K., Wu L., et al., Acidity Regulation for Improved Activity of Mo/HZSM-5 Catalyst in Methane Dehydroaromatization, *Chemical Engineering Science*, **266:** 118289 (2023).

[45] Sun H., Cao L., Zhang Y., Zhao L., Gao J., Xu C., Effect of Catalyst Acidity and Reaction Temperature on Hexene Cracking Reaction to Produce Propylene, *Energy Fuels*, **35:** 3295−3306 (2021).

[46] Lee Y., Kim E., Kim J.R., Kim J.W., Kim T.W., Chae H.J., et al., The Effect of K and Acidity of NiW-Loaded HY Zeolite Catalyst for Selective Ring Opening of 1-Methylnaphthalene, *Journal of Nanoscience and Nanotechnology*, **16:** 4335–4341 (2016).

[47] Jensen K.H., Sigman M.S., Evaluation of Catalyst Acidity and Substrate Electronic Effects in a Hydrogen Bond-Catalyzed Enantioselective Reaction, *Journal of Organo Chemistry*, **75:** 7194–7201(2010).

[48] Jian-Lu Z., Xin-Ping W., Ke-Gong F., Tian-Xi C., Mo-Jiea C., Xin-He B., Effect of Support and Acidity of Catalyst on the Direct Oxidation of Ethylene to Acetic Acid, *Reaction Kinetics and Catalysis Letters*, **73:** 13-20 (2001).

[49] Viscardi R., Barbarossa V., Gattia D.M., Maggi R., Maestri G., Pancrazzi F., Effect of Surface Acidity on the Catalytic Activity and Deactivation of Supported Sulfonic Acids during Dehydration of Methanol to DME, *New Journal of Chemistry, Issue* **44:** 16810-16820 (2020).

[50] Ali M., Roozbahani G., Ziarati M., Khandan N., Methanol Steam Reforming; Effects of Various Metal Oxides on the Properties of a *Cu*-based Catalyst, *Iranian Journal of Hydrogen & Fuel Cell*, **4:** 291–9 (2016).

[51] Khandan N., Kazemeini M., Aghaziarati M., Determining an Optimum Catalyst for Liquid-Phase Dehydration of Methanol to Dimethyl Ether, *Applied Catalysis A: General*, **349:** 6–12 (2008).